Theoretical and Experimental Evaluation of Detached Endcaps for Birdcage Coils

M. ALECCI[1], J. L. WILSON[1], P. JEZZARD[1], W. LIU[2], C. M. COLLINS[2], M. B. SMITH[2]
[1]University of Oxford, FMRIB Centre, Oxford, United Kingdom; [2]Pennsylvania State University, Center for NMR Research, Hershey, USA;

INTRODUCTION

At low field (≤1.5T) the use of an endcap improves the axial RF B1 homogeneity of head-size birdcage coils [1-3]. Usually, endcaps are made of a very large copper foil that is an integral part of the service end of the RF coil (permanent endcap). For functional MRI studies which use head insert gradient coils the RF coil must be located within the gradient coil (diameter<38cm). This makes the size of the endcap comparable to the birdcage diameter, and previous analytical models for calculating the B1 distribution cannot be applied. Recently, a Finite Difference Time Domain (FDTD) analysis of the effect of endcap diameter for 1.5T birdcage coils was reported [4]. However, only permanent endcaps were considered and the RF shield was not included in the FDTD model of the coil. The use of a detached endcap for birdcage coils was recently suggested to improve the axial RF homogeneity [5]. However, only a simplified Biot-Savart analysis was described and no experimental data were reported.

AIMS

We have investigated the use of a detached endcap for a 3T birdcage coil. FDTD analysis, work-bench and MRI techniques were used to map the axial B1 distribution without and with the endcap present, and include the effects of the RF shield.

METHODS AND RESULTS

Endcap Design

Our 3T Varian MRI system is equipped with a 16 element quadrature birdcage coil [6]. The RF coil diameter and length are 278mm and 221mm, respectively. A cylindrical RF copper shield (dia 380mm, length 254mm, thickness 5um) was used. The center of the RF shield is shifted 16mm toward the patient end of the coil. A detached endcap, made of copper foil (dia 380mm, thickness 35um) and fixed on an acrylic disk, was built (Fig. 1). The resonant frequency and the Q of the birdcage without and with the endcap were measured with a network analyser (HP8712C). Because of mutual inductive coupling, the endcap increased the resonant frequency of the birdcage by up to 1.5MHz (within the tuning range of the birdcage). No appreciable variation of the Q was observed. For workbench calibration, the endcap was positioned at d=13mm or d=19mm from the RF shield (service end) and the axial B1 amplitude was measured using an oscilloscope (HP54610B) and a small pick-up coil.

FDTD Simulation

A 16-leg low-pass birdcage coil, shield, and endcap were modelled with nearly the same dimensions and relative locations as used in the experiment [7]. The model was created on a 3D grid with 4mm resolution in the x- and y-oriented directions and with 2.5mm resolution in the z-oriented (parallel to coil axis) direction. Exact replication of the experiment was not possible due to the discrete nature of the FDTD method. Distances between the endcap and the shield were 12.5 and 20mm from the end of the shield. Other distances nearer to and farther from the shield (including the case for no endcap) were also modelled. The coil model was shielded asymmetrically, with the service end of both the coil and the shield being at the same z coordinate (z=0). Steady-state solutions of the transverse (x-y) B1 field magnitude along the axis of the coil were calculated at 128MHz with the FDTD method [8].

FDTD and Workbench Results

Workbench (squares) and FDTD (continuous line) axial B1 maps of the empty birdcage coil without the endcap present are reported in Fig. 2. The B1 field showed a severe inhomogeneity, with the maximum B1 at 11cm from the service end (z=0cm). At the service end itself the B1 value was only about 45%. In Fig. 2 are also shown the B1 maps obtained with the endcap at d=13mm (triangles and dotted line) and d=19mm(circles and dashed line). Workbench and FDTD data show a good agreement (maximum difference <10%). We found that the detached endcap improves the B1 distribution and at the service end the B1 amplitude is about 85% (d=13mm). As expected, the B1 on the patient side of the coil was practically unaffected by the presence of the endcap. FDTD calculations suggest that a better axial B1 distribution could be obtained with d<13mm. With the present birdcage prototype a shorter endcap to shield distance could not be tested. However, for very small distances a large detuning of the birdcage is expected.

MRI Results

Spin-echo images (TR=1.5s, TE=20ms) with volunteers were obtained without and with the endcap (d=13mm), see Fig. 3. An MRI signal plot (average of 4 slices) along the central line of the sagittal images is reported in Fig. 4. A significant improvement of the MRI signal distribution was observed with the endcap present. This is in qualitative agreement with the workbench and FDTD data, taking into account the presence of anatomical structures.

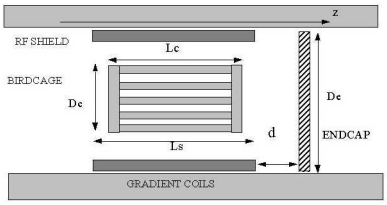

Fig. 1 Diagram of the endcap, birdcage and gradient coils.

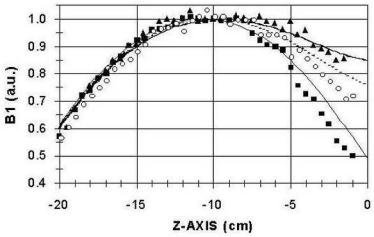

Fig. 2 Calculated and experimental B1 field magnitudes along axis of birdcage for different locations of endcap.

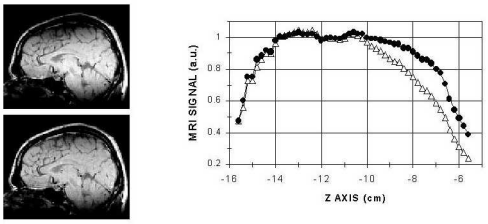

Fig. 3 Spin-echo images obtained without (top) and with (bottom) the endcap. Experimental MRI signal amplitude in human head along axis of coil without (triangles) and with endcap (circles).

CONCLUSIONS

We have shown that a detached RF endcap is effective in improving the axial B1 distribution of a 3T birdcage coil. This endcap design is simple to implement and allows a versatile use of birdcage coils for fMRI studies, where in particular conditions full access to the coil's service end is required. With EPI pulse sequences, additional eddy currents can be induced on the endcap by the switching gradient coils. However, strategies to reduce or eliminate eddy currents are well known [5].

REFERENCES

1. Hayes, C.E., *Proc. ISMRM,* page 39, 1986.
2. Wong, E.C., *et al*, *Proc. ISMRM,* page 4015, 1992.
3. Chen, J., *et al*, *Proc. ISMRM,* page 2041, 1998.
4. Hadley, J.R., *et al*, *Proc. ISMRM*, 8, 1409, 2000.
5. Jin, J., "EM Analysis and Design in MRI", CRC, 1999.
6. Barberi, E.A., *et al*, *MRM*, 43, 284, 2000.
7. Collins, C.M., *et al*, *MRM*, 40, 847, 1998.
8. Yee, K.S., *IEEE Trans. Ant. Propag.* 14, 302, 1966.